

Analysis of transient processes in a power supply system of concentrated and distributed parameters based on variational approaches

Abstract. Starting with variational approaches using a modified Hamilton-Ostrogradsky principle, a mathematical model of a power system is developed and analysed as a concentrated parameters system for power autotransformer feeder reactors and capacitors and as a distributed parameters system for supply lines. The final discretised state equations of the power system are represented in Cauchy format. Results of computer simulations are presented as drawings.

Streszczenie. Korzystając z podejść wariacyjnych przy użyciu zmodyfikowanej zasady Hamiltona-Ostrogradzkiego, opracowano matematyczny model systemu elektroenergetycznego, który analizuje się jako układ o parametrach rozproszonych. Końcowe, dyskretyzowane równania stanu systemu elektroenergetycznego są przedstawione w formie Cauchy'ego. Wyniki symulacji komputerowych przedstawiono na rysunkach. (Analiza procesów niustalonych w układzie elektroenergetycznym o parametrach skupionych i rozłożonych na podstawie podejść wariacyjnych).

Keywords: Hamilton-Ostrogradsky principle, interdisciplinary modelling, power system, power supply line, distributed parameters system, telegraph equation, concentrated and distributed parameters system.

Słowa kluczowe: zasada Hamiltona-Ostrogradzkiego, modelowanie interdyscyplinarne, system elektroenergetyczny, linia zasilania, równanie telegrafistów, układ o parametrach skupionych i rozłożonych.

Introduction

Application of mathematical apparatus to modelling of electrical power systems is virtually the most effective method. This approach finds extensive applicability in the case of power systems including long supply lines.

Such a system generally consists of widely different parts: power plants, switching stations, supply lines, compensation systems, and a number of other elements [1]. Long power supply lines are key parts in electricity processing and transmission. High voltage lines between local power systems constitute inter-system connections. Fault currents, dependent inter alia on capacitances between wires, and leakage currents, which depend on electric charges on wire surfaces (corona discharge), must be considered in these lines. Current in line wires generates an alternating magnetic field that induces along a self-induction SEM line. In addition, voltage between the line wires is not constant either. To address current and voltage variations along the line, it must be assumed each infinitely short wire section exhibits resistance and inductance, with capacitance and conductance between wires of that section. In other words, the line should be treated as a distributed parameters system [2].

In view of these conditions, use of ordinary and partial differential equations, including the telegraph equation, is recommended for analysis of transient processes in power systems. Their solution is not a problem. Both analytical and numerical methods are employed (D'Alembert's, Fourier's, reticulated, and other methods.) Finding boundary conditions for the telegraph equation as parts of the only system of general differential equations of a power system is the most complicated problem in analysis of transient processes in power systems, on the other hand. The theory of applied mathematics says Dirichlet first type, Neuman second type, and Poincaré third type boundary conditions serve to solve boundary problems [3]. Boundary conditions of the first type are commonly used to solve the telegraph equation in specialist publications [4]. This approach is reasonable if functional dependences (charge, current or voltage, depending on the type of telegraph equation [3]) at a line's start and terminal are known. In actual problems of applied electrical engineering, meanwhile, these functional

dependences at line terminals are unknown, for instance, in analysis of complicated elements of power subsystems connected with long lines. Since boundary conditions are normally not known openly in our studies [3], the first-type condition cannot be utilised.

Another approach, including the boundary conditions of the second and third types, is necessary to solve real, complex power systems. This will employ not functional dependences but spatial functional derivatives, as well as equations of these functions. Use of Neuman and Poincaré conditions allows for exclusion of e.g. voltage from a system of discretised differential equations in fictitious discretisation nodes, reducing them to a single system of differential equations where the number of unknowns is the same as the number of equations.

From the viewpoint of mathematical modelling, two approaches are commonly applied to analysis of transient processes in dynamic systems: classic and variational – in our case interdisciplinary. As part of the former, a sole dynamic system is analysed as a combination of non-stationary systems. For example, power engineering and mechanical equations are combined by means of equations relating equilibrium of moments [1, 3, 5, 6, 7]). The defect of this method is obvious: relational equations cannot be fully solved in distributed parameters systems, which in turn restricts adequacy of the integrated system model. This defect does not apply to the variational approaches in [3], where a new interdisciplinary method is developed modifying Hamilton-Ostrogradsky principle by expanding the Lagrange function with two components: energy of dissipation and energy of external non-potential forces. This modification of the principle of least action allows for applying the variational approach that is fully comparable to classic approaches [3].

The objective of this study is to develop a method of analysing transient processes in complicated power systems of concentrated and distributed parameters based on variational approaches.

Mathematical model of the system

A power system shown in Fig. 1 is used in connection with transient processes in this article. A three-phase supply

line with the default voltage of 750 kV in its single-phase and single-line version is the central element of the system.

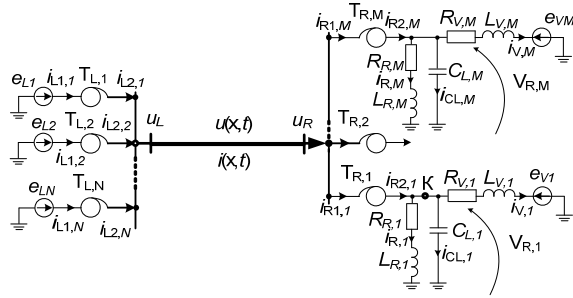


Fig. 1. Circuit diagram of a local power system

N sources of infinite power are connected to the left side of the line by means of non-linear power autotransformers with a transformation coefficient of 750/330. T_R autotransformers in Figure 1 operate as an electricity receiver shown as M equivalent networks of the default voltage 400 kV. This system is addressed as a concentrated parameter arrangement. Symmetrisation of the system's operating conditions, including those of a 400 kV supply system, is a key issue. Air-spaced coils are added to the system, therefore, in order to symmetrise its operation.

Hamilton-Ostrogradsky action functional [3] for the system in Fig. 1 is as follows:

$$(1) \quad S = \int_{t_1}^{t_2} \left(L^* + \int_l L_l dl \right) dt, \quad I = \int_l L_l dl,$$

where S – Hamilton-Ostrogradsky actions, I – energetic functional, L_l – linear density of the modified Lagrangian and its corresponding linear densities of all the foregoing energies.

$$(2) \quad L^* = \tilde{T}^* - P^* + \Phi^* - D^*,$$

where L^* – modified Lagrangian, \tilde{T}^* – kinetic energy (coenergy), P^* – potential energy, Φ^* – energy of generalised dissipation forces, D^* – energy of lateral non-potential forces.

$$(3) \quad T^* = \sum_{j=1}^N \left(\int_0^{i_{L1,j}} \Psi_{L1,j} di_{L1,j} + \int_0^{i_{L2,j}} \Psi_{L2,j} di_{L2,j} \right) + \sum_{j=1}^M \left(\int_0^{i_{R1,j}} \Psi_{R1,j} di_{R1,j} + \int_0^{i_{R2,j}} \Psi_{R2,j} di_{R2,j} + \frac{L_{R,j} i_{R,j}^2}{2} + \frac{L_{V,j} i_{V,j}^2}{2} \right), \quad P^* = \sum_{j=1}^M \frac{Q_{CL,j}^2}{2C_{L,j}};$$

$$(4) \quad \Phi^* = \frac{1}{2} \sum_{j=1}^N \int_0^t (r_{L1,j} i_{L1,j}^2 + r_{L2,j} i_{L2,j}^2) d\tau + \frac{1}{2} \sum_{j=1}^M \int_0^t (r_{R1,j} i_{R1,j}^2 + r_{R2,j} i_{R2,j}^2 + R_{R,j} i_{R,j}^2 + R_{V,j} i_{V,j}^2) d\tau;$$

$$(5) \quad D^* = \frac{1}{2} \sum_{j=1}^N \int_0^t (e_{L,j} i_{L1,j} + u_L i_{L2,j}) d\tau +$$

$$+ \frac{1}{2} \sum_{j=1}^M \int_0^t (u_R i_{R1,j} - V_{R,j} i_{R2,j} + e_{V,j} i_{V,j}) d\tau;$$

$$(6) \quad \frac{\partial T^*}{\partial x} \equiv T_l = \frac{L_0 i^2}{2}, \quad \frac{\partial P^*}{\partial x} \equiv P_l = \frac{1}{2C_0} Q_x^2, \quad Q_x \equiv \frac{\partial Q}{\partial x}, \quad Q_t \equiv \frac{\partial Q}{\partial t} = i(x,t);$$

$$(7) \quad \frac{\partial \Phi^*}{\partial x} \equiv \Phi_l = \Phi_{I3} - \Phi_{IB} = \int_0^t \left(\frac{R_0}{2} Q_t^2 - \frac{g_0}{2C_0^2} Q_x^2 \right) \Big|_{t=\tau} d\tau,$$

where: L – left-hand side index of power supply to the line, R – right-hand side index of power supply to the line, Ψ – associated streams, i – currents, $i(x, t)$ – current across the line, R_0, g_0, C_0, L_0 – line parameters, Φ_{R3} – dissipation of external energy, Φ_{RB} – dissipation of internal energy, $Q(x, t)$ – load on the line, N, M – number of autotransformers; $e(t)$ – electromotive forces; $L_{V,M}$ – total inductances of the line and of the electric power system; $L_{R,M}$ – inductances of air-spaced coils; $R_{V,M}$ – total resistances of the line and of the electric power system; $R_{R,M}$ – resistances of air-spaced coils; C_{L1}, C_{L2} – capacitances of the line; Q_{CL1}, Q_{CL2} – electric loads for capacitors C_{L1}, C_{L2} ; $r_{R1,j}, r_{R2,j}, r_{L1,j}, r_{L2,j}$ – resistances of the primary and secondary power autotransformer windings.

Solving (1) – (7) – see examples in [8, 9] – produces Euler-Lagrange equations:

$$(8) \quad \frac{d\Psi_{L1,j}}{dt} = e_{L,j} - r_{L1,j} i_{L1,j}, \quad \frac{d\Psi_{L2,j}}{dt} = u_L - r_{L2,j} i_{L2,j}, \quad j=1, \dots, N;$$

$$(9) \quad \frac{d\Psi_{R1,j}}{dt} = u_R - r_{R1,j} i_{R1,j}, \quad \frac{d\Psi_{R2,j}}{dt} = V_{R,j} - r_{R2,j} i_{R2,j}, \quad j=1, \dots, M;$$

$$(10) \quad \frac{du_{CL,j}}{dt} = \frac{i_{CL,j}}{C_{L,j}}, \quad u_{CL,j} = V_{R,j}, \quad j=1, \dots, M;$$

$$(11) \quad \frac{di_{R,j}}{dt} = \frac{1}{L_{R,j}} (u_{CL,j} - R_{R,j} i_{R,j}), \quad j=1, \dots, M;$$

$$(12) \quad \frac{di_{V,j}}{dt} = \frac{1}{L_{V,j}} (V_{R,j} - R_{V,j} i_{V,j} - e_{V,j}), \quad j=1, \dots, M.$$

$$(13) \quad \frac{\partial v(x,t)}{\partial t} = (C_0 L_0)^{-1} \left(\frac{\partial^2 u}{\partial x^2} - (g_0 L_0 + C_0 R_0) v - g_0 R_0 u \right), \quad \frac{\partial u}{\partial t} = v,$$

Ψ -model of the autotransformers will be converted into an appropriate A-type model [3]:

$$(14) \quad \frac{di_{L1,j}}{dt} = A_{11L,j} (e_{L,j} - r_{L1,j} i_{L1,j}) + A_{12L,j} (u_L - r_{L2,j} i_{L2,j}), \quad j=1, \dots, N;$$

$$(15) \quad \frac{di_{L2,j}}{dt} = A_{21L,j} (e_{L,j} - r_{L1,j} i_{L1,j}) + A_{22L,j} (u_L - r_{L2,j} i_{L2,j}), \quad j=1, \dots, N;$$

$$(16) \quad \frac{di_{R1,j}}{dt} = A_{11R,j} (u_R - r_{R1,j} i_{R1,j}) + A_{12R,j} (V_{R,j} - r_{R2,j} i_{R2,j}), \quad j=1, \dots, M;$$

$$(17) \quad \frac{di_{R2j}}{dt} = A_{21R,j}(u_R - r_{R1j}i_{R1j}) + A_{22R,j}(V_{R,j} - r_{R2j}i_{R2j}), \quad j = 1, \dots, M;$$

where $A_{km,j}$ – coefficients dependent on reverse inductances of power autotransformers [3].

$$(18) \quad A_{11} = \frac{\alpha_{\sigma 1}(\alpha_{\sigma 2} + \rho)}{\alpha_{\sigma 1} + \alpha_{\sigma 2} + \rho}, \quad A_{12} = A_{21} = -\frac{\alpha_{\sigma 1}\alpha_{\sigma 2}}{\alpha_{\sigma 1} + \alpha_{\sigma 2} + \rho};$$

$$(19) \quad A_{22} = \frac{\alpha_{\sigma 2}(\alpha_{\sigma 1} + \rho)}{\alpha_{\sigma 1} + \alpha_{\sigma 2} + \rho}, \quad \rho = \frac{\partial i_m}{\partial V_m}, \quad i_m = i_1 + i_2.$$

where i_1, i_2 – currents across primary and secondary autotransformer windings.

Relations among the line elements will be formulated taking the second Kirchhoff's law for distributed parameter electric circuits as the starting point [2, 3]

$$(20) \quad -\frac{\partial u(x,t)}{\partial x} = R_0 i(x,t) + L_0 \frac{\partial i(x,t)}{\partial t}.$$

Equations (13) and (20) are then discretised using the straight line method (central derivative) [1]

$$(21) \quad \frac{dv_j}{dt} = (C_0 L_0)^{-1} \left(\frac{u_{j-1} - 2u_j + u_{j+1}}{(\Delta x)^2} - (g_0 L_0 + C_0 R_0)v_j - g_0 R_0 u_j \right), \quad \frac{du_j}{dt} = v_j, \quad j = 1, \dots, N;$$

$$(22) \quad -\frac{u_{j+1} - u_{j-1}}{2\Delta x} = R_0 i_j + L_0 \frac{di_j}{dt}, \quad j = 1, \dots, N.$$

By solving (10) – (12), (14) – (17) together with (21), (22), the following will then result:

$$(23) \quad u_0 = \frac{2\Delta x L_0}{3} \left\{ \sum_{j=1}^N (A_{21L,j}(e_{L,j} - r_{L1j}i_{L1j}) + A_{22L,j}(u_1 - r_{L2j}i_{L2j})) - \Delta x g_0 v_1 - \frac{\Delta x}{L_0} \left[\frac{1}{(\Delta x)^2} (-2u_1 + u_2) - (g_0 L_0 + C_0 R_0)v_1 - g_0 R_0 u_1 \right] + \frac{1}{L_0} \left(\frac{u_2}{2\Delta x} + R_0 i_1 \right) \right\}.$$

$$(24) \quad u_{N+1} = u_{N-1} - 2(u_N - u_R).$$

$$(25) \quad u_R = \left(\frac{1}{\Delta x L_0} + \sum_{j=1}^M A_{11R,j} \right)^{-1} \left(\frac{u_N}{\Delta x L_0} - \frac{R_0}{L_0} i_N + \sum_{j=1}^M (A_{11R,j} r_{R1j} i_{R1j} - A_{12R,j} (V_{R,j} - r_{R2j} i_{R2j})) \right).$$

Node voltages $V_{r,j}$ will now be determined, see Fig. 1.

$$(26) \quad \frac{dV_{R,j}}{dt} = \frac{du_{CL,j}}{dt} = \frac{i_{R2,j} - i_{V,j} - i_{R,j}}{C_{L,j}}, \quad j = 1, \dots, M.$$

The line currents will be obtained by discretisation (20) using the straight line method, though now by means of the right-side derivative [3]:

$$(27) \quad \frac{di_j}{dt} = \frac{1}{L_0 \Delta x} (u_j - u_{j+1}) - \frac{R_0}{L_0} i_j, \quad j = 1, \dots, N-1.$$

The system of equations: (11), (12), (14) – (17), (21), (26), (27) will be jointly integrated owing to (18), (19), (23) – (25).

Results of computer simulations

A computer simulation of transient processes was applied to the instance of the power system illustrated in Figure 1 assuming $N = M = 2$. Where the system operates in a steady state, symmetrical three-phase short-circuiting takes place on the side of voltage 400 kV (K in Fig. 1, $t = 0.2$ s). The system's parameters: $e_{L1} = 622\sin(\omega t + 0^\circ)$ kV, $e_{L2} = 619\sin(\omega t + 2.3^\circ)$ kV, $e_{R1} = 581\sin(\omega t + 11.9^\circ)$ kV, $e_{R2} = 593\sin(\omega t + 14.9^\circ)$ kV, $r_{TL1} = r_{TL2} = 0.98 \Omega$, $L_{TL1} = L_{TL2} = 0.188$ H, $r_{TR1} = r_{TR2} = 0.95$ Ohm, $L_{TR1} = L_{TR2} = 0.184$ H, $R_{V,1} = 4.805 \Omega$, $L_{V,1} = 0.189$ H, $C_{L,1} = 1.1399 \cdot 10^{-6}$ F, $R_{V,2} = 4.267 \Omega$, $L_{V,2} = 0.163$ H, $C_{L,2} = 0.7979 \cdot 10^{-6}$ F, $R_{R,1} = R_{R,2} = 5.58 \Omega$, $L_{R,1} = L_{R,2} = 472$ H. The line is 476 km long, while: $R_0 = 1.9 \cdot 10^{-5} \Omega / \text{m}$, $L_0 = 9.24 \cdot 10^{-7}$ H/m, $C_0 = 1.3166 \cdot 10^{-11}$ F/m, $g_0 = 3.25 \cdot 10^{-11}$ Sm/m.

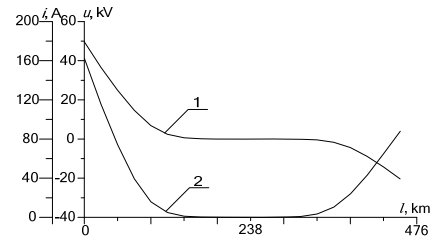


Fig. 2. Distribution of space voltage (1) and current (2) distribution across the supply line for the time $t = 0.0005$ s

Distribution of space voltage (1) and current (2) across the supply line is presented in Figure 2. Note the highly complex process of an electromagnetic wave expanding along the line. The voltage in the initial line section is 45kV, at the terminal -20kV, whereas it is zero in the middle part of the line.

Figures 3 and 4 show temporary current and voltage in the middle section of the supply line when loaded.

At the instant $t = 0$ s, all the existing SEMs were connected to the system and the amplitude of the voltage function in the steady process reached 620 kV, with current – 0.7 kA.

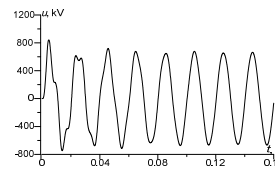


Fig. 3. Temporary voltage in the middle of the line

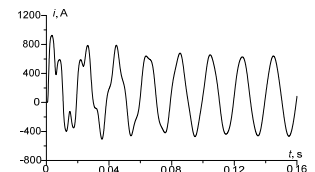


Fig. 4. Temporary current in the middle of the line

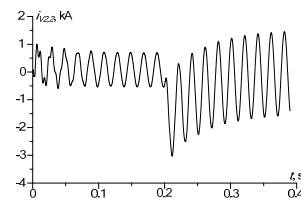


Fig. 5. Current $i_{R2,2}$ of the autotransformer $T_{R,2}$ 750/400 kV.

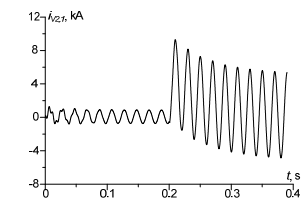


Fig. 6. Current $i_{R2,1}$ of the autotransformer $T_{R,1}$ 750/400 kV.

Analysis of Figures 5 and 6 shows the temporary currents across the power autotransformer windings on the side of 400 kV contain aperiodic components. This is related to presence of shunt short-circuit reactors on the 400 kV side. On short-circuiting ($t = 0.2$ s), the short-

circuiting current $i_{R2,2}$ of $T_{R,2}$ reaches 3 kA and $i_{R2,1}$ of $T_{R,1}$ reaches the value of 9.4 kA.

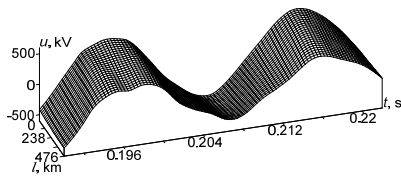


Fig. 7. Temporal-spatial distribution of the voltage function within the time range $t \in [0.19; 0.24]$ s.

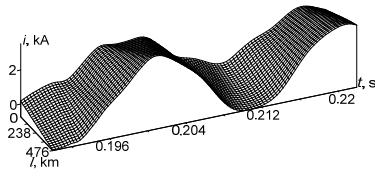


Fig. 8. Temporal-spatial distribution of the current function within the time range $t \in [0.19; 0.24]$ s.

Figures 7 and 8 contain spatial waveforms of voltage and current. They are very important from a user's point of view, since they indicate temporal-spatial distribution of the waveforms after short-circuiting. A physical effect – motion of an electromagnetic wave along a supply line – can also be seen in Figures 7 and 8.

Conclusion

1. Application of modified Hamilton-Ostrogradsky principle to mathematical modelling of dynamic systems, including power systems, allows for describing an integrated power system with equations relying on a single energetic approach only.
2. Finding initial and, in particular, boundary conditions is an important part of solving boundary or mixed problems. Boundary conditions of the second and third types need to be employed to search for the latter in power systems.
3. Results of computer simulations enable analysis of dynamic states, of use at the stages of design and operation of power facilities.
4. Graphs of complicated functional dependences in supply lines should be presented in 3D space. Such graphics allow for analysis of electromagnetic wave motion in space and time.

Authors: dr Andriy Chaban, Eng., University of Technology and Humanities, Faculty of Transport and Electrical Engineering, Malczewskiego 29, 26-600 Radom, e-mail: atchaban@gmail.com; dr Marek Lis, Eng., Czestochowa University of Technology, Faculty of Electrical Engineering, al. Armii Krajowej 17, e-mail: lism@el.pcz.czest.pl; dr inż. Andrzej Szafraniec, University of Technology and Humanities, Faculty of Transport and Electrical Engineering, ul. Malczewskiego 29, 26-600 Radom, e-mail: a.szafraniec@uthrad.pl; dr Marcin Chrzan, Eng., University of Technology and Humanities, Faculty of Transport and Electrical Engineering, ul. Malczewskiego 29, 26-600 Radom, e-mail: m.chrzan@uthrad.pl; Vitaliy Levoniuk, MSc Eng., Lviv National Agrarian University, W. Wielkiego 1, Lviv, e-mail: Bacha1991@ukr.net.

REFERENCES

- [1] Rusek A., Stany dynamiczne układów napędowych z silnikami indukcyjnymi specjalnego wykorzystania, *Wydawnictwo Politechniki Częstochowskiej*, Częstochowa, (2012)
- [2] Simoni K., *Theoretische elektrotechnik*. – Berlin, (1956)
- [3] Chaban A., Principle Gamiltona-Ostrogradskiego in elektromechanicznych systems, *Soroki Lviv*, (2015), 488
- [4] Kyrylenko O. V., Sergey M. S., Butkevich O. F., Mazur T. A., Modelowanie matematyczne w elektrotechnice, *Lwów, Narodowy Uniwersytet "Politechnika Lwowska"*, (2010), 608
- [5] Lis M., Modelowanie matematyczne procesów niestabilnych w elektrycznych układach napędowych o złożonej transmisji ruchu, *Wydawnictwo Politechniki Częstochowskiej*, (2013), 258
- [6] Łukasik Z., Czaban A., Szafraniec A., Mathematical model of asynchronous pump drive with distributed mechanical parameters, *Przegląd Elektrotechniczny*, R.94 nr. 6 (2018), 155-159
- [7] Szafraniec A., Modelowanie matematyczne procesów oscylacyjnych w napędzie elektrohydraulicznym o podatnej transmisji ruchu, *Przegląd Elektrotechniczny*, R.93 nr. 12 (2017), 167-171
- [8] Czaban A., Lis M., Sosnowski J., Lewoniuk W., Mathematical model of the double conductor power line using a modified Hamilton's principle. *Electric machines*, nr. 109, (2016), 31 – 36
- [9] Czaban A., Lis M., Chrzan M., Szafraniec A., Levoniuk V., Mathematical modelling of transient processes in power supply grid with distributed parameters. *Przegląd Elektrotechniczny*, nr. 1, (2018), 17 – 20
- [10] White D.C., Woodson H.H., *Electromagnetic Energy Conversion*, New-York, John Wiley & Sons, Inc, (1958)
- [11] Buslova NV, Vinnoslavsky VN, Denisenko G.I., Perchach VS., *Electrical networks and systems*, Ed. Denisenko, High school, (1986), 584
- [12] Czaban A., Szafraniec A., Lis M., Levoniuk V., Lysiak H., Figura R., Transient Processes Analysis in a Part of an Power Grid during a Automatic Reclosing Cycle, *Control of Power Systems 13th International Scientific Conference CPS 2018*, Tatraské Matliare - Tatraská Lomnica, 5-7 June 2018